Quantifying low levels (<0.5% w/w) of warfarin sodium salts in oral solid dose forms using Transmission Raman spectroscopy

Julia A.Griffen, Andrew W.Owen
and Pavel Matousek

Published version information

Citation: JA Griffen, AW Owen and P Matousek. "Quantifying low levels (<0.5% w/w) of warfarin sodium salts in oral solid dose forms using Transmission Raman spectroscopy." Journal of Pharmaceutical and Biomedical Analysis, vol. 155 (2018): 276-283.

DOI: 10.1016/j.jpba.2018.04.008

Quantifying low levels (<0.5% w/w) of Warfarin sodium salts in oral solid dose forms using Transmission Raman Spectroscopy

Julia A. Griffen[a*], Andrew W. Owen[a], Pavel Matousek[b].

[a] Agilent Technologies Ltd, 174 Brook Drive, Milton Park, Abingdon, Oxfordshire, OX14 4SD, UK

[b] Central Laser Facility, Research Complex at Harwell, STFC Rutherford Appleton Laboratory, Harwell Oxford, OX11 0QX, UK

*Corresponding Author: Julia.Griffen@Agilent.com

Keywords: Transmission Raman; Warfarin; Raman Spectroscopy; Crystallinity; Polymorphism

Abstract

In this feasibility study Transmission Raman spectroscopy (TRS) has been used to build quantitative models for Warfarin sodium and Warfarin sodium clathrate. The type of warfarin present in manufactured tablets may affect product quality. Models were used to predict warfarin sodium in commercially available tablets at extremely low dosage levels (0.5% w/w). The laboratory made calibration samples used in the modelling varied in amorphous sodium, crystalline clathrate warfarin forms, excipients and dye. This application was highly challenging due to the low level of API and high level of a Raman-active colourant which varied significantly between production batches. A photon recycling optic, known as a Beam Enhancer, was utilised to improve the signal to noise of the Raman spectra to attain a low limit of quantification of 0.19% w/w.

1 Introduction

1.1 Introduction to warfarin

Warfarin, a coumarin derivative, is an anticoagulant that reduces the formation of blood clots and is used to treat patients to reduce the risk of strokes, heart attacks and other thromboembolic conditions. Warfarin is administered orally and is available in either a liquid solution or in a solid dose form. It is the most prescribed oral anticoagulant and one of the most prescribed medicines in the US [1]. Warfarin is available in 9 dose strengths ranging from 1 mg up to 10 mg. This large range is needed as the treatment has a narrow therapeutic range, the dose response is genetically determined and varies significantly from patient to patient [2].

Pure warfarin is most readily available as a salt, either in its amorphous form of Warfarin sodium (WS) or a crystalline form as Warfarin sodium clathrate (WSC). WSC is a dimer of two warfarin molecules bridged by an isopropylalcohol (IPA) moiety. WSC is used in commercial formulations. WSC decomposes with the loss of IPA to WS at high (>68% RH) humidity [3]. Traditional chromographic assay methods, *e.g.* high-performance liquid chromatography (HPLC) cannot be used to differentiate between WSC and WS as in solution the species are identical.

Previous work has shown that the presence of WS polymorphic forms affect product quality [4]. Further studies suggest that manufacturing variables can influence crystallinity of WSC and hence affect critical quality attributes such as dissolution time [5]. It is therefore critically important to control and measure the crystalline WSC content of the drug form in the final solid dose product and throughout the products lifetime from manufacture to patient.

1.2 Transmission Raman Spectroscopy

TRS was pioneered by Schrader in early days [6]. The technique remained relatively unutilised, until ~ 2006, from which point it has seen several applications towards pharmaceutical analysis [7,8]. Initial work made comparisons with conventional backscatter geometry Raman techniques [9,10]. Pharmaceutical samples including powders, tablets and capsules were analysed demonstrating the improved accuracy of whole sample analysis and how the reduction in subsampling improves quantitative model performance [11,12]. As with any other Raman based technology TRS tends to be non-destructive. The transmission geometry adds favourable characteristics of bulk sampling [13,14] and the ability to measure the whole intact final dosage form avoids sample preparation steps.

Solvation states and polymorphic forms have been extensively studied using Raman based technologies [15,16]. There are a few notable examples that utilise TRS; initial work showed the expected benefit of superior quantification compared to backscatter geometries [17,18]. Further work compared TRS to NIR, with TRS achieving marginally better quantitative model performance statistics [19]. TRS has also been used to quantify the amount of amorphized material in a polymer tablets after microwave irradiation, al be it a high >10% w/w drug loading [20]. A brief study compared TRS to XRD and ssNMR in spray dried solid dispersions, critically evaluating both performance and suitability for routine testing. TRS demonstrated a limit of detection (LOD) comparable with the ssNMR method (0.9% w/w) al be it with a measurement time of seconds and without the need to alter the sample in any way [21]. The most recent work demonstrated the capability of quantifying low (0.62 - 1.32% w/w) levels of polymorph content, and additionally the sole decomposition and transformation from one form to another while the excipient content remained constant [22].

Previous work has demonstrated the use of beam enhancer technology with TRS to improve signal to noise and/or speed of data acquisition of TRS measurements [22]. The Beam Enhancer is a dielectric bandpass filter that reflects laser radiation back towards the sample, the majority of which scatters away from the sample and would otherwise reduce the number of photons able to scatter through the sample matrix. This results in the sample being exposed to more laser radiation overall and hence leads to a higher Raman yield in the TRS geometry.

1.3 Previous work on warfarin

NIR reflectance has been described for the quantitative determination of WS, combining both laboratory and production tablets in a through calibration and experimental approach at dose strengths from 1 to 10 mg [23]. The same authors later demonstrated Raman spectroscopy as a complimentary method for Content uniformity of break-scored warfarin tablets between 1 and 10 mg dose strengths [24]. Warfarin crystallinity analysis work demonstrated the application of NIR chemometric methods to quantification of warfarin sodium products. Samples at 4 and 10% w/w warfarin content subsequently ranged between 0 - 100% of both WSC and WS form. This thorough study demonstrated the importance and viability of spectroscopic techniques for warfarin crystallinity quantification [25].

Another study from the FDA [26] successfully used Raman and ^{13}C NMR to quantify 5% warfarin (varying from 0 - 100%) in a formulation of common pharmaceutical excipients. The study concluded

'The developed chemometric models based on Raman spectroscopy provides easy and fast method for quantifying WS amorphous/crystalline fraction in the drug products.'

However, Warfarin dose strengths typically range from 1 to 10 mg and this corresponds to, in tablets that are ~200 mg in mass, 0.5 to 5% w/w content range. Previous studies have successfully demonstrated both NIR, Raman and ssNMR technologies but only for the higher dose strengths.

In this work we have concentrated on the lowest dose strength 1 mg (0.5% w/w). This is additionally challenging as the commercial available formulations of interest contain a red organic dye that has a very strong Raman scattering cross section and is present in approximately the same content (~0.4% w/w) as the API. Formulations from different vendors (US) contain the same dye and only distinguishable via shape [27]. The dye content may vary from batch to batch and because it is such a strong Raman active species this could affect quantitative predictions using Raman techniques.

This is the first TRS crystalline quantification study that uses lab made calibration samples to predict commercially available pharmaceutical products at such low dosage levels. This feasibility study sets TRS as a viable technology for crystallinity determination of oral solid dose forms.

2 Materials and Methods

2.1 Materials

The formulation contained Warfarin sodium (WS), Warfarin sodium clathrate (WSC), lactose monohydrate, pregelatinized corn starch, dye (colour D&C RED #6 barium lake), magnesium stearate. All chemicals were purchased from Sigma Aldrich, UK.

Commercial and placebo samples were supplied from a pharmaceutical manufacturer (anonymity requested).

2.2 Preparation

Calibration samples were prepared using a fractional cubic design of experiment (DoE) as per Figure 1 and Table 1. This approach was followed to minimise the number of samples and to include variation of the dye content, which is a strong Raman scatterer and varies between production batches. Centre point of the DoE assumed that of the production formulation 0.5% w/w WSC (1 mg in a 200 mg tablet). Calibration samples were made from powders weighed and mixed manually with a pestle and mortar and compressed into 8 mm flat rounds under consistent pressure using a die set and manual tablet press with adjustable pressure gauge. Individual tablets were consistently weighed between 195 to 205

mg, Seven tablets were pressed per calibration sample point. Production tablets were 11 mm elliptical/oval tablets weighting between 198 to 202 mg. Production samples were predominantly flat with slight biconvex/bevelled edges, both sides were embossed with commercial information.

Spectra were collected on a TRS100 (Agilent Technologies Ltd, UK). The system operates using an 830nm laser with an automated sample tray to analyse multiple samples in one experimental run. Tablets were analysed using the photon recycling optic placed in a 'Beam Enhancer tray' (Agilent Technologies Ltd, UK). The principle of the Raman signal enhancing effect has been described previously [28]. Acquisition settings were: 4mm laser beam diameter at sample, 650 mW laser power with low-area collection optics. Tablets were scanned for 50 accumulations at 0.4 seconds corresponding to approximately 30 seconds scan per tablet.

Calibration data were collected in triplicates for 7 tablets per sample (19 samples) resulting in 399 TRS spectra. Independent validation samples containing the WSC product were analysed under the same acquisition settings, consisting of 7 tablets per batch (4 production + 1 placebo) were collected in triplicate resulting in 105 spectra. There was very little difference in total signal from calibration and validation despite difference in size and shape.

2.3 Chemometric Analysis

Multivariate, chemometric analysis was performed in Solo (Eigenvector Research Inc., Wenatchee, WA, US). Model building followed the process as described extensively [29]. SIMPLS algorithm was used as default within the software using a multi Y block for quantitative modelling, the features of SIMPLS has been described extensively [30]. Previous work involving TRS data showed very little difference between single and multi Y block PLS1 and PLS2 analysis [31]. Model building pre-processing consisted of 1st derivative, normalisation (each variable divided by the sum of the absolute value of all variables for the given sample) followed by mean centring over the spectral region shown in Figure 3.

3 Results and Discussion

Pure API spectra, calculated spectral differences and the dye spectra are shown in Figure 2. Spectra are consistent with that previously described [26]. Both WS and WSC are strong Raman active species with distinct peaks around 680, 1002, 1030, 1422, 1480, 1606 and 1660 cm^{-1}. Spectral differences

between the crystalline WSC versus WS are observed at approximately 680, 1034, 1426 and 1610 cm^{-1}. The dye spectrum, which is a red organic dye, exhibits a strong Raman response with features between 1300 – 1700 cm^{-1}. Due to the overlap between the dye and the API, the dye has been built into the DoE design and varied over five levels. Table I.

Table I: DoE Formulation values in % w/w. Colour = D&C red #6 barium lake, Starch = pregelatinized corn starch.

Sample	Warfarin sodium	Warfarin clathrate	Colour	Starch	Mag. Stearate	Lactose
1	0.35	-	0.41	7.31	1	90.9
2	0.39	-	0.32	8.85	1	89.4
3	0.39	-	0.32	5.77	1	92.5
4	0.50	-	0.29	7.31	1	90.9
5	0.50	-	0.53	7.31	1	90.7
6	0.61	-	0.50	8.85	1	89.1
7	0.61	-	0.32	5.77	1	92.3
8	0.65	-	0.41	7.31	1	90.6
9	0.50	-	0.41	7.31	1	90.8
10	-	0.38	0.41	7.31	1	90.9
11	-	0.43	0.50	8.85	1	89.2
12	-	0.43	0.50	5.77	1	92.3
13	-	0.55	0.29	7.31	1	90.9
14	-	0.55	0.53	7.31	1	90.6
15	-	0.66	0.32	8.85	1	89.2
16	-	0.66	0.50	5.77	1	92.1
17	-	0.71	0.41	7.31	1	90.6
18	-	0.55	0.41	7.31	1	90.7
19	0.25	0.27	0.41	7.31	1	90.8

Figure 3 shows the calibration spectra (19 samples x 7 tablets x 3 repeats = 399 spectra) with the spectral regions used for model building. The spectra show distinct Raman features with low levels of background fluorescence. The wavenumber region <500 cm^{-1} was purposefully over-exposed during measurements, and therefore avoided in model building, to improve the signal quality towards the higher wavenumber region. Wavenumber range between 850-950 cm^{-1} was also removed as this showed marginally better performance as part of the method development process.

Figure 4 a and b indicates a specific Raman region (~675 cm^{-1}) with two Raman bands, one corresponding to WSC and the other to WS, demonstrating that differences between the two salt forms in the final blended calibration samples are observed.

The resulting PLS calibration models are shown in Figure 5, with corresponding latent variables shown in Figure 6. The PLS models were used to predict commercial validation samples, tablets from four different production batches and placebo tablets shown in Figure 10.

157 The PLS models were built using a multi Y block SIMPLS algorithm. Internal cross-validation was
158 performed automatically within the model building software with no grouping of repeated
159 measurements. By taking this approach, the PLS model should be insensitive to repeated
160 measurements of the same sample and minute shifts in wavenumber and intensity due to
161 photobleaching.
162 Four latent variables were selected for model building as this showed best performance without
163 overfitting. Considering there are four strong Raman active species (WS, WSC, Dye and Lactose)
164 present in the calibration set it is reasonable to select four latent variables to build the models.
165 Both models exhibit linearity with R^2 = 0.99 across a range of +/- 30% of the nominal API concentration.
166 Their RMSE-C and -CV are approximately 0.018% w/w. The notable similarity between RMSE-C and
167 CV indicates good model stability between adding and removing samples as part of internal cross
168 validation, and suggested the model isn't overfitted and the number of latent variables chosen (4) is
169 appropriate. Model accuracy can be estimated by taking the RMSECV and comparing it to the model
170 'middle' (~0.55% w/w) results in a relative 'error' value of approximately 3%.
171 Specificity can be ascertained by comparison of the latent variables to the pure component spectra
172 shown in Figure 6 and through analysis of the scores plot. Figure 7 indicates that latent variable 1
173 separates out WSC and WS samples and trends with concentration of each form, with features at 682,
174 1026 and 1607 cm^{-1}. Figure 8a indicates that latent variable 2 corresponds to dye variation with strong
175 features around 1300-1600 cm^{-1}. The high percentage (76%) of latent variable 2 shows how spectrally
176 dominant the dye is within the calibration sample set. Figure 8b indicates that latent variable 4 trends
177 with the difference between repeated measurements, the weighting of this variable is very low <1%. In
178 terms of repeatability and reproducibility this indicates there are some spectral differences within a
179 sample and between repeated measurement, but the differences are indistinguishable between such
180 factors and relatively small. The approach taken to include all spectra in one model should in theory
181 result in a model that is insensitive to individual and repeated measurement differences. Figure 9
182 indicates that latent variable 3 trends with concentration of API independent of WSC and WS
183 concentration, with key peaks around 680, 1020 and 1600 cm^{-1}.
184 Statistical estimation of the limit of detection (LOD) in multivariate calibration is a complex problem and
185 has been discussed previously [32]. For this work we have followed a simplified ICH recommendation
186 where the LOD can be estimated from the PLS linear regression following the calculation of (3.3 x

standard deviation of the residual error)/slope of the regression. Results indicate values of 0.06% w/w for both WS and WSC. Limit of Quantification can be estimated from the PLS linear regression following the calculation of (10 x standard deviation of the residual error)/slope of the regression. Results indicate values of 0.19% w/w for WS and WSC.

Validation samples predicted results are shown in Figure 10. The results indicate, as expected, that the production samples contain WSC and no detectable WS. The results also predict the placebo to contain no WSC or WS. The model RMSEP values are slightly higher suggesting a 5% error (0.0285% w/w RMSEP /0.55% w/w).

4 Conclusions

This study by its initial outlay and design is by no means comprehensive, with a relatively small calibration sample set and limited availability of validation samples. This type of study will also be limited by a comparative reference technology, with HPLC unsuitable for differentiating between WS and WSC, we have had to assume the samples were made up accurately.

However, the study demonstrated feasibility and suitability of TRS to quantifying low levels of WSC and WS in solid oral dose forms of the lowest commercially available dose strength, between 0.25 to 0.71% w/w, at levels not previously demonstrated. Results indicate spectral differences between the warfarin salt forms, and quantitative models for each of the salt forms can be built with good accuracy and limit of detection estimated to 0.06% w/w. Validation of model performance was assed via cross validation and independent production quality tablets with respective relative errors of 2% and 5%.

Additionally, noteworthy is that the calibration sample set contained only laboratory made round tablets, which was used to predict different size and shape production quality samples. This ease of use and insensitivity to physical parameters infers the robustness of the TRS technique.

This sets TRS as a viable technology for analysis of pharmaceutical final dosage forms – quantifying low levels of API's in a fast-non-destructive manner. Setting a precedence, moving away from the proof of concept space and towards that of industrially applicable TRS measurements.

5 Acknowledgements

Work was carried out by Agilent Technologies Ltd. UK who provided materials resource and instrumentation. The commercial partner whom supplied production material wished to remain anonymous, but approved publication of this work with their name omitted.

Figure Captions

Figure 1: Design of Experiment (DoE) sample space, centric cubic design consisting of 19 samples.

Figure 2: Pure API spectra of WS and WSC, dye spectra and calculated difference between the warfarin salts.

Figure 3: Calibration Spectra selected regions used for model building.

Figure 4a and 4b: Zoomed in region of baseline and normalised calibration spectra looking at peak ~680 cm^{-1} where clear differences between clathrate and sodium Warfarin content can be observed.

Figure 5: PLS calibration models for WSC and WS/

Figure 6: PLS model Latent Variables plotted alongside WS and WSC spectra.

Figure 7: Scores plots showing latent variable 1 separates out concentration of API coloured by WS and WSC.

Figure 8a and 8b: Coloured according to dye content trends with Latent variable 2 (8a). Coloured by WS content, latent variable 4 correlates with repeated measurements (8b).

Figure 9a and 9b: Latent Variable 3 trends with concentration of API independent of WS (9a) and WSC (9b).

Figure 10: Validation Samples predictions

References

[1] B. Bikdeli, A. Gupta, P. Mody, J.F. Lampropulos, K. Dharmarajan, Most Important Outcomes Research Papers on Anticoagulation for Cardiovascular Disease, Circ. Cardiovasc. Qual. Outcomes. 5 (2012) e65–e74. doi:10.1161/CIRCOUTCOMES.112.968701.

[2] S. Stehle, J. Kirchheiner, A. Lazar, U. Fuhr, Pharmacogenetics of oral anticoagulants: a basis for dose individualization., Clin. Pharmacokinet. 47 (2008) 565–94. http://www.ncbi.nlm.nih.gov/pubmed/18698879 (accessed June 2, 2016).

[3] D. Gao, M.B. Maurin, Physical chemical stability of warfarin sodium, AAPS PharmSci. 3 (2001) 18–25. doi:10.1208/ps030103.

[4] L.M. Vercaigne, G.G. Zhanel, Clinical significance of bioequivalence and interchangeability of narrow therapeutic range drugs: focus on warfarins., J. Pharm. Pharm. Sci. 1 (1998) 92–4. http://www.ncbi.nlm.nih.gov/pubmed/10948395 (accessed June 2, 2016).

[5] Z. Rahman, M. Korang-Yeboah, A. Siddiqui, A. Mohammad, M.A. Khan, Understanding effect of formulation and manufacturing variables on the critical quality attributes of warfarin sodium product, Int. J. Pharm. 495 (2015) 19–30. doi:10.1016/j.ijpharm.2015.08.065.

[6] B. Schrader, G. Bergmann, Die Intensitat des Ramanspektrums polykristalliner Substanzen, Fresenius' Zeitschrift Fur Anal. Chemie. 225 (1967) 230–247. doi:10.1007/BF00983673.

[7] J.A. Griffen, A.W. Owen, D. Andrews, P. Matousek, Recent advances in pharmaceutical analysis using transmission Raman spectroscopy, Spectroscopy. 32 (2017) 37–43.

[8] K. Buckley, P. Matousek, Recent advances in the application of transmission Raman spectroscopy to pharmaceutical analysis, J. Pharm. Biomed. Anal. 55 (2011) 645–652. doi:10.1016/j.jpba.2010.10.029.

[9] N. Kellichan, A. Nordon, P. Matousek, D. Littlejohn, G. McGeorge, Variation in the transmission near-infrared signal with depth in turbid media., Appl. Spectrosc. 68 (2014) 383–7. doi:10.1366/13-07002.

[10] R. Takeshima, Y. Hattori, S. Managaki, M. Otsuka, Analysis of the dehydration process of caffeine using backscattering and transmission Raman spectroscopy, Int. J. Pharm. 530 (2017) 256–262. doi:10.1016/J.IJPHARM.2017.07.082.

[11] M.D. Hargreaves, N. a. Macleod, M.R. Smith, D. Andrews, S. V. Hammond, P. Matousek, Characterisation of transmission Raman spectroscopy for rapid quantitative analysis of intact multi-

component pharmaceutical capsules, J. Pharm. Biomed. Anal. 54 (2011) 463–468. doi:10.1016/j.jpba.2010.09.015.

[12] Y. Li, B. Igne, J.K. Drennen, C.A. Anderson, Method development and validation for pharmaceutical tablets analysis using transmission Raman spectroscopy, Int. J. Pharm. 498 (2016) 318–325. doi:10.1016/j.ijpharm.2015.11.049.

[13] P. Matousek, N. Everall, D. Littlejohn, A. Nordon, M. Bloomfield, Dependence of signal on depth in transmission Raman spectroscopy, Appl. Spectrosc. 65 (2011) 724–733. doi:10.1366/11-06259.

[14] N. Everall, P. Matousek, N. MacLeod, K.L. Ronayne, I.P. Clark, Temporal and Spatial Resolution in Transmission Raman Spectroscopy, Appl. Spectrosc. 64 (2010) 52–60.

[15] C.J. Strachan, T. Rades, K.C. Gordon, J. Rantanen, Raman spectroscopy for quantitative analysis of pharmaceutical solids., J. Pharm. Pharmacol. 59 (2007) 179–192. doi:10.1211/jpp.59.2.0005.

[16] M. Korang-Yeboah, Z. Rahman, D.A. Shah, M.A. Khan, Spectroscopic-Based Chemometric Models for Quantifying Low Levels of Solid-State Transitions in Extended Release Theophylline Formulations, J. Pharm. Sci. 105 (2016) 97–105. doi:10.1016/j.xphs.2015.11.007.

[17] C. McGoverin, M.D. Hargreaves, P. Matousek, K.C. Gordon, Pharmaceutical polymoprh quantified with tranmission Raman spectrscopy, J. Raman Spectrosc. 43 (2012) 280–285.

[18] L. Netchacovitch, E. Dumont, J. Cailletaud, J. Thiry, C. De Bleye, P.-Y. Sacré, M. Boiret, B. Evrard, P. Hubert, E. Ziemons, Development of an analytical method for crystalline content determination in amorphous solid dispersions produced by hot-melt extrusion using transmission Raman spectroscopy: A feasibility study, Int. J. Pharm. 530 (2017) 249–255. doi:10.1016/J.IJPHARM.2017.07.052.

[19] M.C. Hennigan, A.G. Ryder, Quantitative polymorph contaminant analysis in tablets using Raman and near infra-red spectroscopies, J. Pharm. Biomed. Anal. 72 (2013) 163–171. doi:10.1016/j.jpba.2012.10.002.

[20] M. Edinger, M.M. Knopp, H. Kerdoncuff, J. Rantanen, T. Rades, K. Löbmann, Quantification of microwave-induced amorphization of celecoxib in PVP tablets using transmission Raman spectroscopy, Eur. J. Pharm. Sci. 117 (2018) 62–67. doi:10.1016/J.EJPS.2018.02.012.

[21] A. Kumar, L. Joseph, J. Griffen, W. Jenny, T. Chi. Y, J. Hau, M. Bloomfield, P. Matousek, L. Wigman, Fast Non-Destructive Detection of Low Level Crystalline Forms in Amorphous Spray Dried Dispersion Using Transmission Raman Spectroscopy and Comparison to Solid-State NMR Spectroscopy, Am.

287 Pharmacetical Rev. (2016).
288 [22] J.A. Griffen, A.W. Owen, J. Burley, V. Taresco, P. Matousek, Rapid quantification of low level polymorph
289 content in a solid dose form using transmission Raman spectroscopy, J. Pharm. Biomed. Anal. 128
290 (2016) 35–45. doi:10.1016/j.jpba.2016.05.017.
291 [23] J. Arruabarrena, J. Coello, S. Maspoch, NIR reflectance determination of warfarin in a solid preparation
292 commercialized at different API mass proportions, Anal. Methods. 5 (2013) 3858.
293 doi:10.1039/c3ay40488a.
294 [24] J. Arruabarrena, J. Coello, S. Maspoch, Raman spectroscopy as a complementary tool to assess the
295 content uniformity of dosage units in break-scored warfarin tablets, Int. J. Pharm. 465 (2014) 299–305.
296 doi:10.1016/J.IJPHARM.2014.01.027.
297 [25] M. Korang-Yeboah, S. Akhtar, A. Siddiqui, Z. Rahman, M.A. Khan, Application of NIR chemometric
298 methods for quantification of the crystalline fraction of warfarin sodium in drug product., Drug Dev.
299 Ind. Pharm. 42 (2016) 584–94. doi:10.3109/03639045.2015.1058817.
300 [26] Z. Rahman, A. Mohammad, S. Akhtar, A. Siddiqui, M. Korang-Yeboah, M.A. Khan, Chemometric Model
301 Development and Comparison of Raman and (13) C Solid-State Nuclear Magnetic Resonance-
302 Chemometric Methods for Quantification of Crystalline/Amorphous Warfarin Sodium Fraction in the
303 Formulations., J. Pharm. Sci. 104 (2015) 2550–8. doi:10.1002/jps.24524.
304 [27] Warfarin Tablet Identification - Anticoagulation Clinic - UC San Diego Health, (n.d.).
305 https://health.ucsd.edu/specialties/anticoagulation/providers/warfarin/Pages/tablet-
306 identification.aspx (accessed February 19, 2018).
307 [28] J. Griffen, A.W. Owen, P. Matousek, Development of Transmission Raman Spectroscopy towards the in
308 line, high throughput and non-destructive quantitative analysis of pharmaceutical solid oral dose.,
309 Analyst. 140 (2015) 107–112. doi:10.1039/c4an01798f.
310 [29] D. Andrews, K. Geentjens, B. Igne, G. McGeorge, A. Owen, N. Pedge, J. Villaumié, V. Woodward,
311 Analytical Method Development Using Transmission Raman Spectroscopy for Pharmaceutical Assays
312 and Compliance with Regulatory Guidelines—Part I: Transmission Raman Spectroscopy and Method
313 Development, J. Pharm. Innov. (2018) 1–12. doi:10.1007/s12247-018-9311-7.
314 [30] S. de Jong, SIMPLS: An alternative approach to partial least squares regression, Chemom. Intell. Lab.
315 Syst. 18 (1993) 251–263. doi:10.1016/0169-7439(93)85002-X.

316 [31] J. Griffen, A.W. Owen, P. Matousek, Comprehensive quantification of tablets with multiple active
317 pharmaceutical ingredients using transmission Raman spectroscopy—A proof of concept study, J.
318 Pharm. Biomed. Anal. 115 (2015) 277–282. doi:10.1016/j.jpba.2015.07.019.
319 [32] F. Allegrini, A.C. Olivieri, IUPAC-Consistent Approach to the Limit of Detection in Partial Least-Squares
320 Calibration, Anal. Chem. 86 (2014) 7858–7866. doi:10.1021/ac501786u.
321

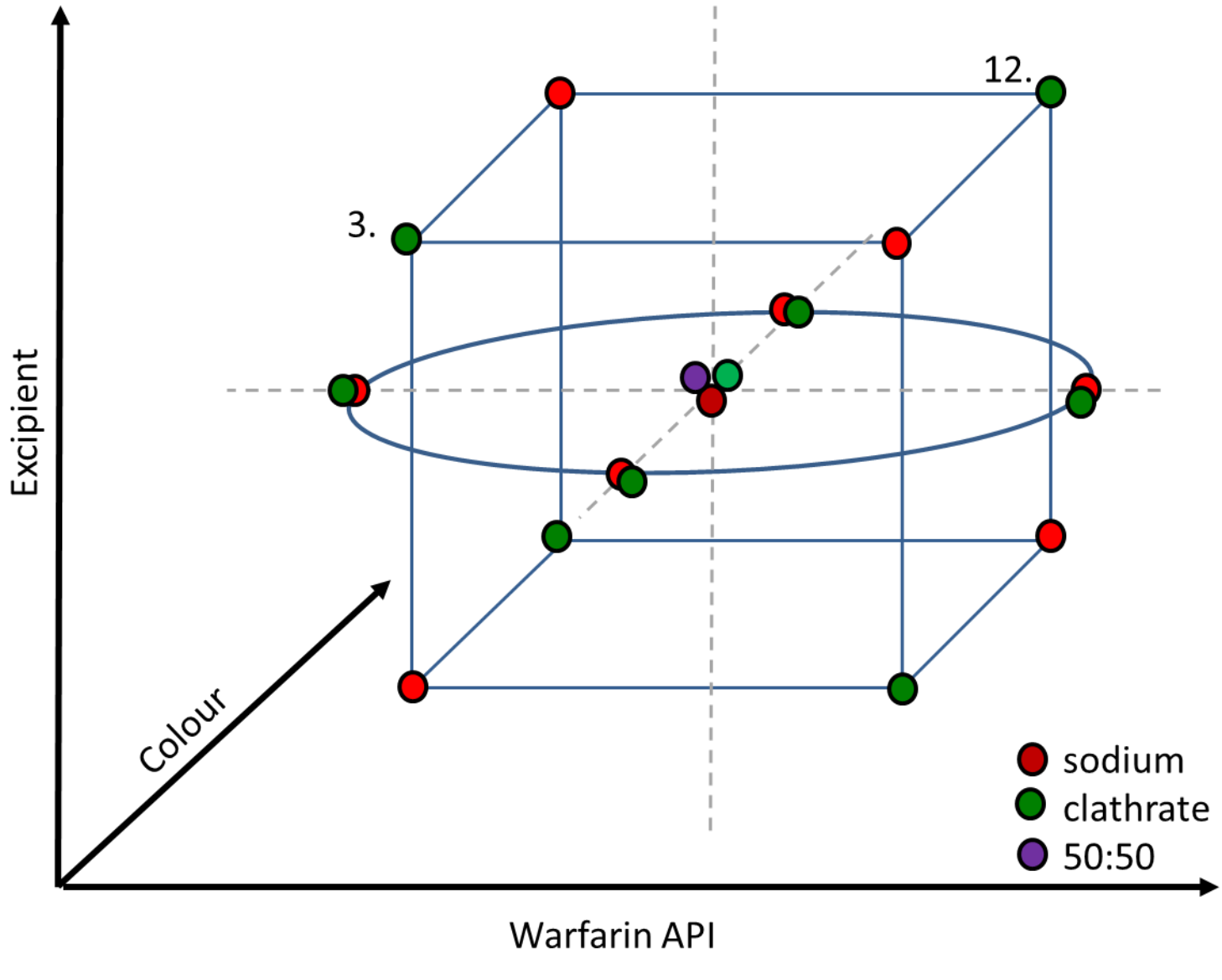
12.
3.
Excipient
Colour
Warfarin API
sodium
clathrate
50:50

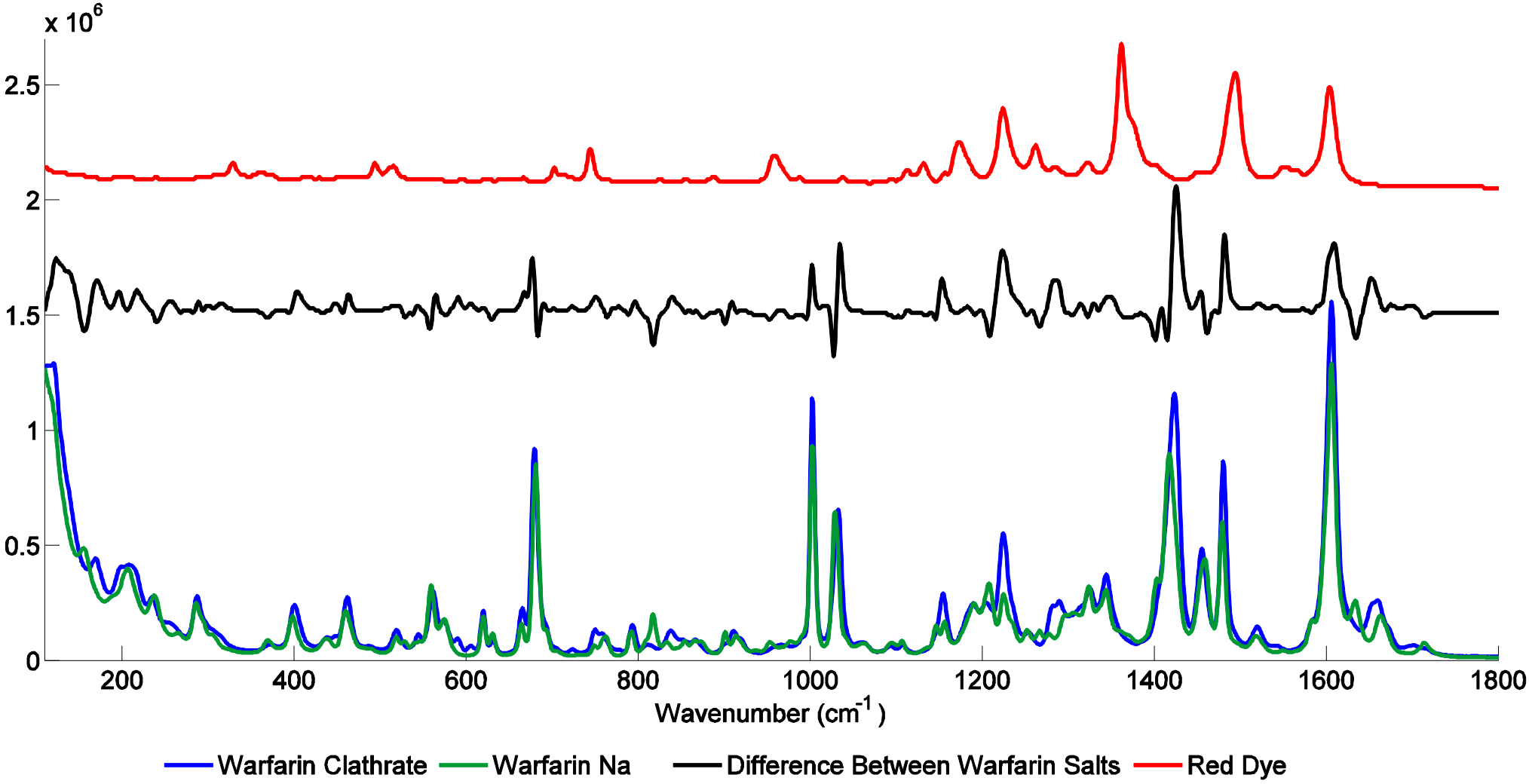
x 10^6
2.5
2
1.5
1
0.5
0
200
400
600
800
1000
1200
1400
1600
1800
Wavenumber (cm^-1)
Warfarin Clathrate
Warfarin Na
Difference Between Warfarin Salts
Red Dye

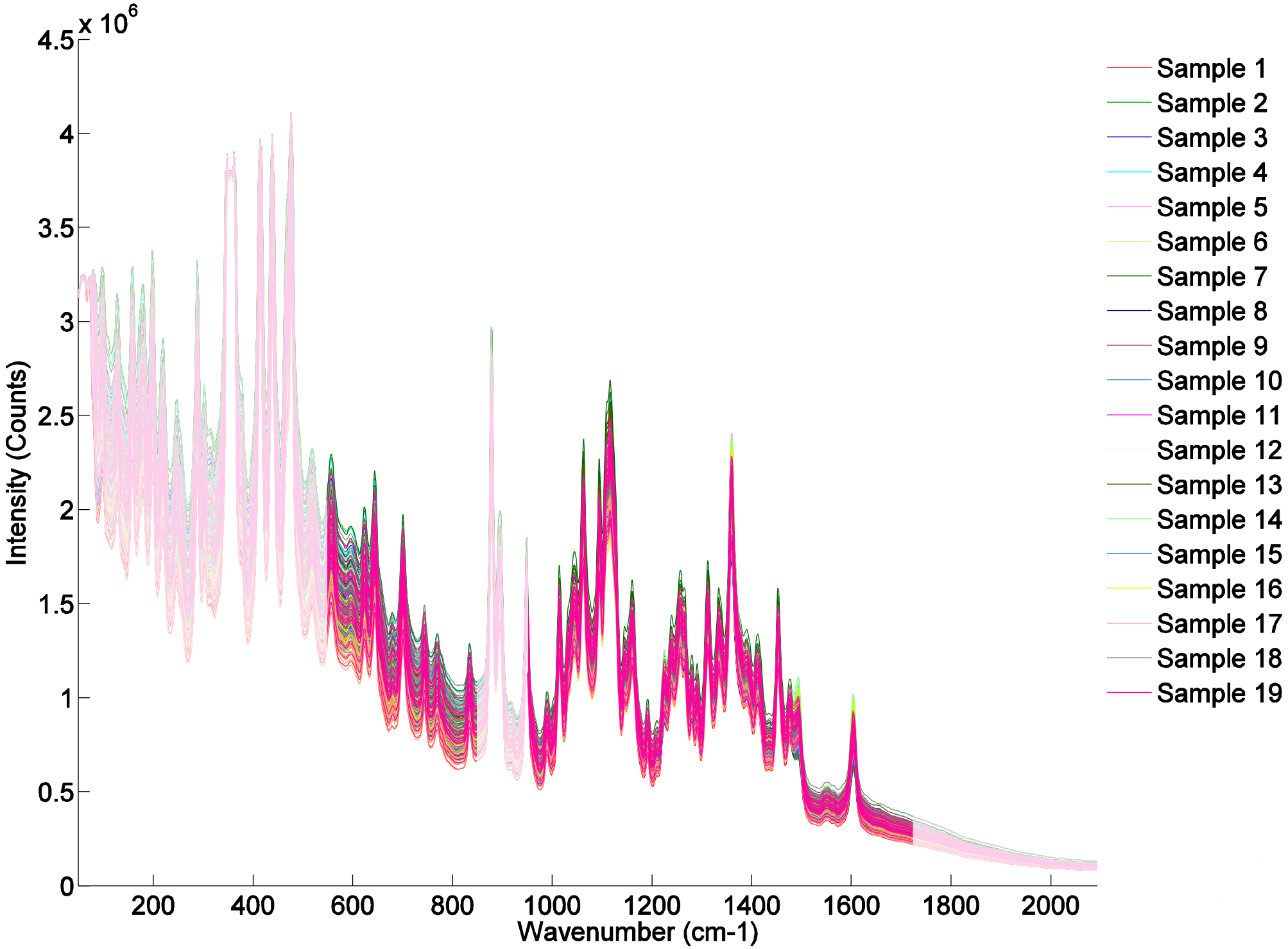
x 10^6
4.5
4
3.5
3
2.5
2
1.5
1
0.5
0
Intensity (Counts)
200
400
600
800
1000
1200
1400
1600
1800
2000
Wavenumber (cm-1)
Sample 1
Sample 2
Sample 3
Sample 4
Sample 5
Sample 6
Sample 7
Sample 8
Sample 9
Sample 10
Sample 11
Sample 12
Sample 13
Sample 14
Sample 15
Sample 16
Sample 17
Sample 18
Sample 19

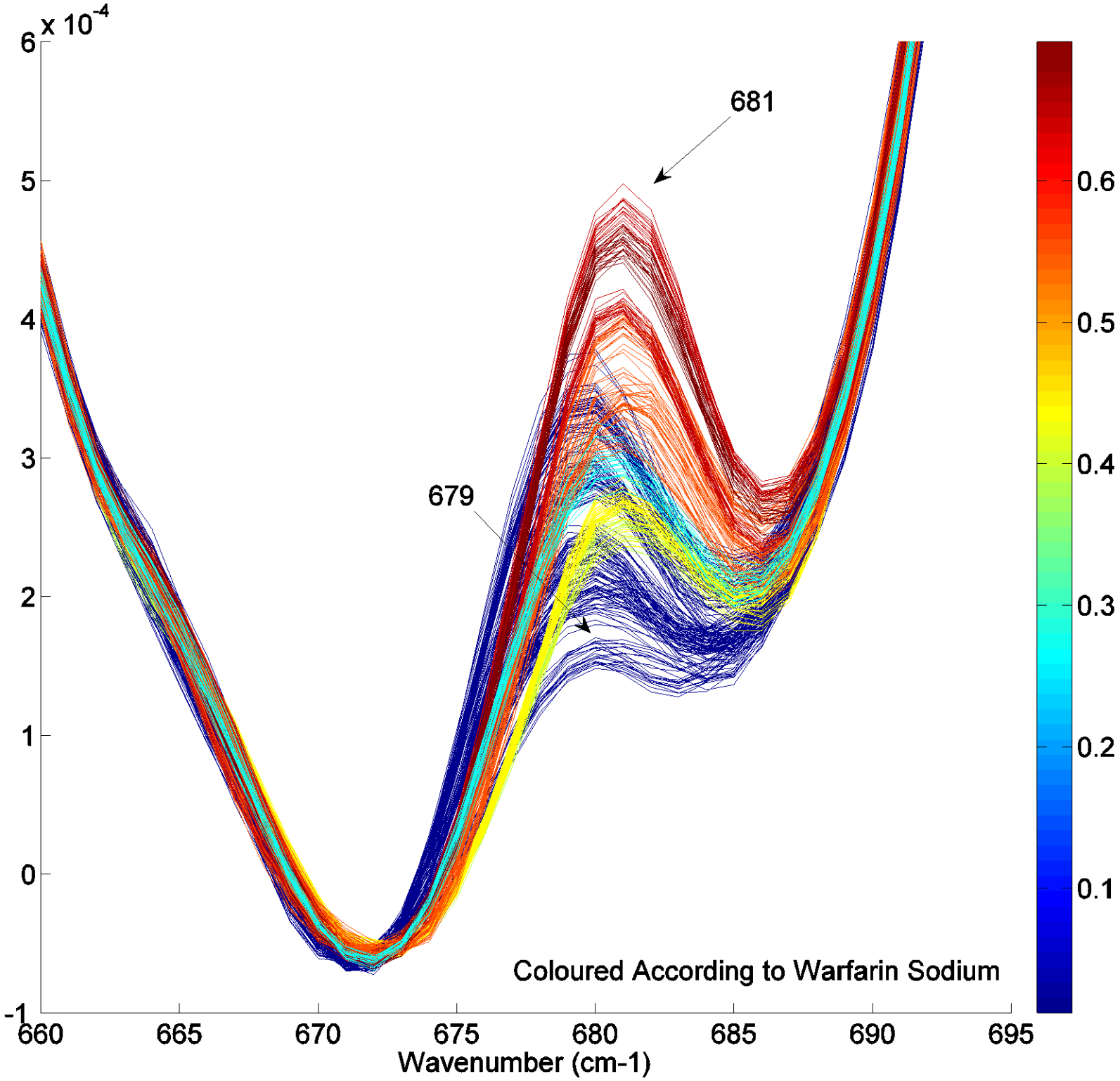
x 10^-4
6
5
4
3
2
1
0
-1
681
679
0.6
0.5
0.4
0.3
0.2
0.1
Coloured According to Warfarin Sodium
660
665
670
675
680
685
690
695
Wavenumber (cm-1)

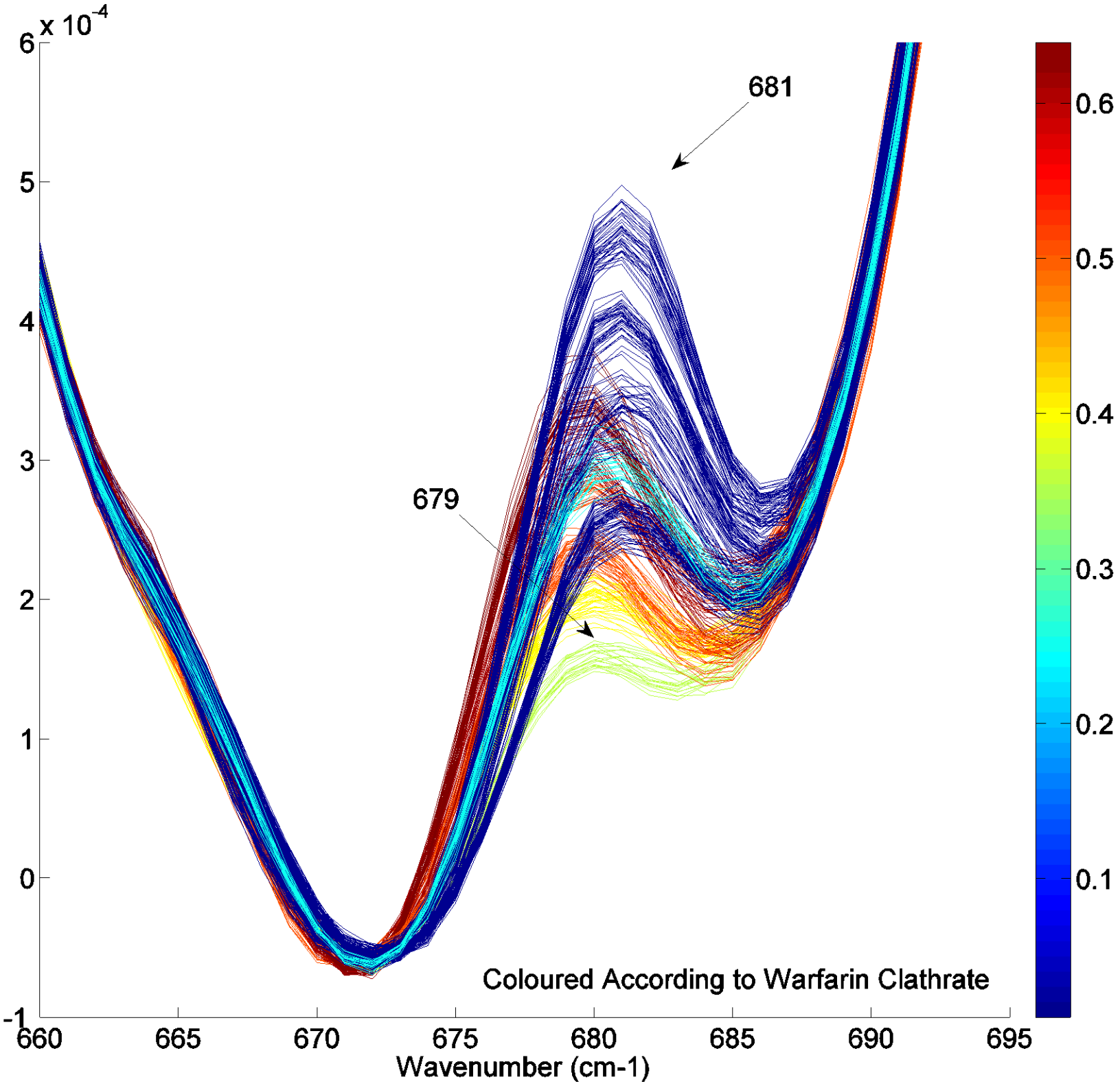
x 10^-4
6
5
4
3
2
1
0
-1
681
679
Coloured According to Warfarin Clathrate
660
665
670
675
680
685
690
695
Wavenumber (cm-1)
0.6
0.5
0.4
0.3
0.2
0.1

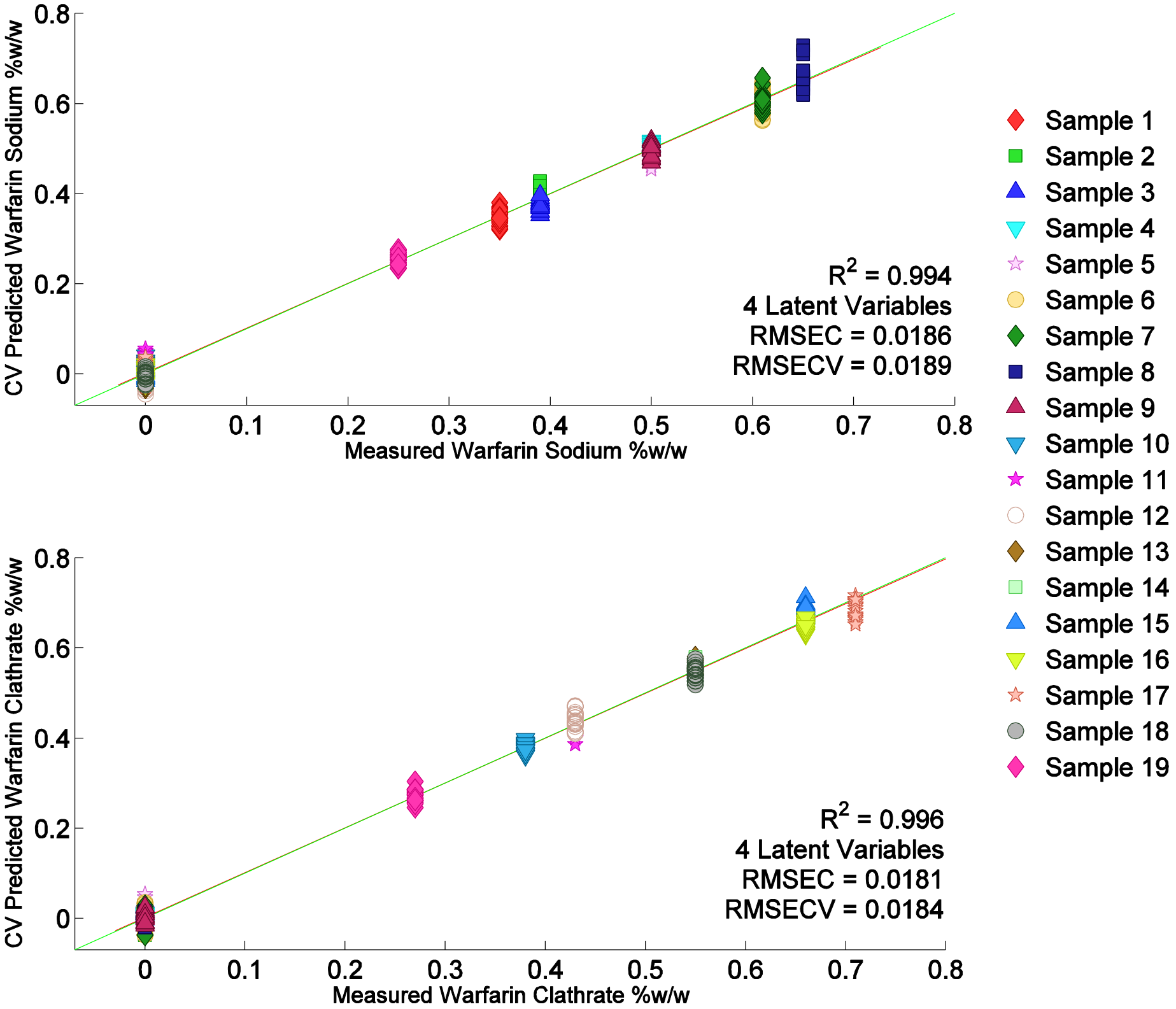
CV Predicted Warfarin Sodium %w/w
Measured Warfarin Sodium %w/w
R2 = 0.994
4 Latent Variables
RMSEC = 0.0186
RMSECV = 0.0189
CV Predicted Warfarin Clathrate %w/w
Measured Warfarin Clathrate %w/w
R2 = 0.996
4 Latent Variables
RMSEC = 0.0181
RMSECV = 0.0184
Sample 1
Sample 2
Sample 3
Sample 4
Sample 5
Sample 6
Sample 7
Sample 8
Sample 9
Sample 10
Sample 11
Sample 12
Sample 13
Sample 14
Sample 15
Sample 16
Sample 17
Sample 18
Sample 19

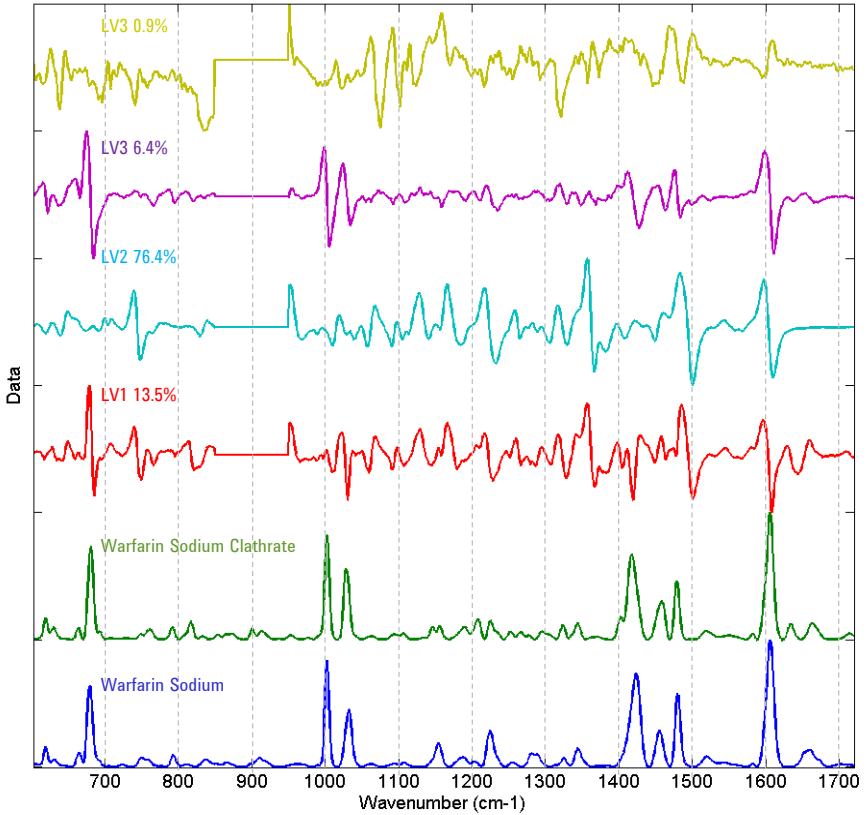
LV3 0.9%
LV3 6.4%
LV2 76.4%
LV1 13.5%
Warfarin Sodium Clathrate
Warfarin Sodium
Data
700
800
900
1000
1100
1200
1300
1400
1500
1600
1700
Wavenumber (cm-1)

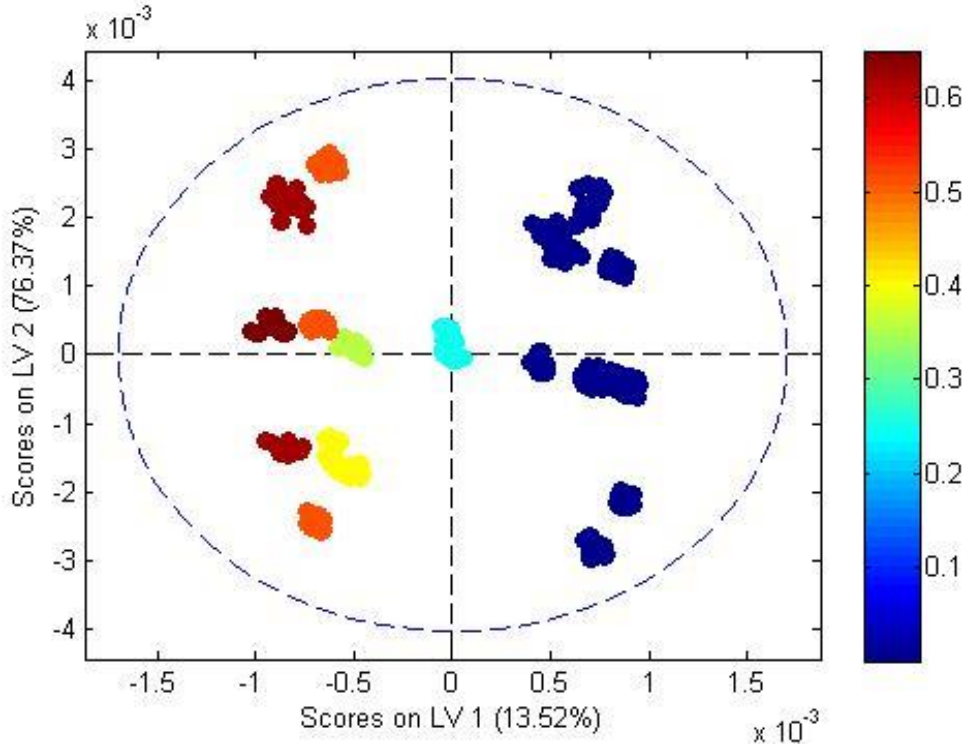
x 10^-3
Scores on LV 2 (76.37%)
Scores on LV 1 (13.52%)
x 10^-3
0.6
0.5
0.4
0.3
0.2
0.1

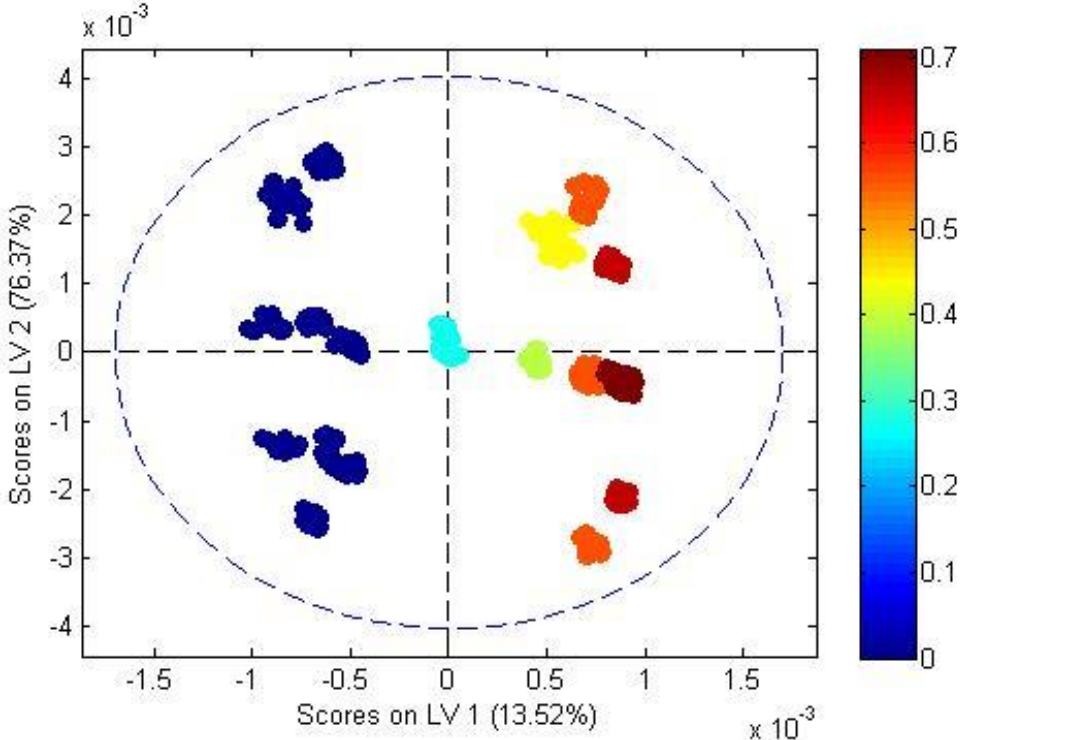
x 10^-3
Scores on LV 2 (76.37%)
Scores on LV 1 (13.52%)
x 10^-3
0.7
0.6
0.5
0.4
0.3
0.2
0.1
0

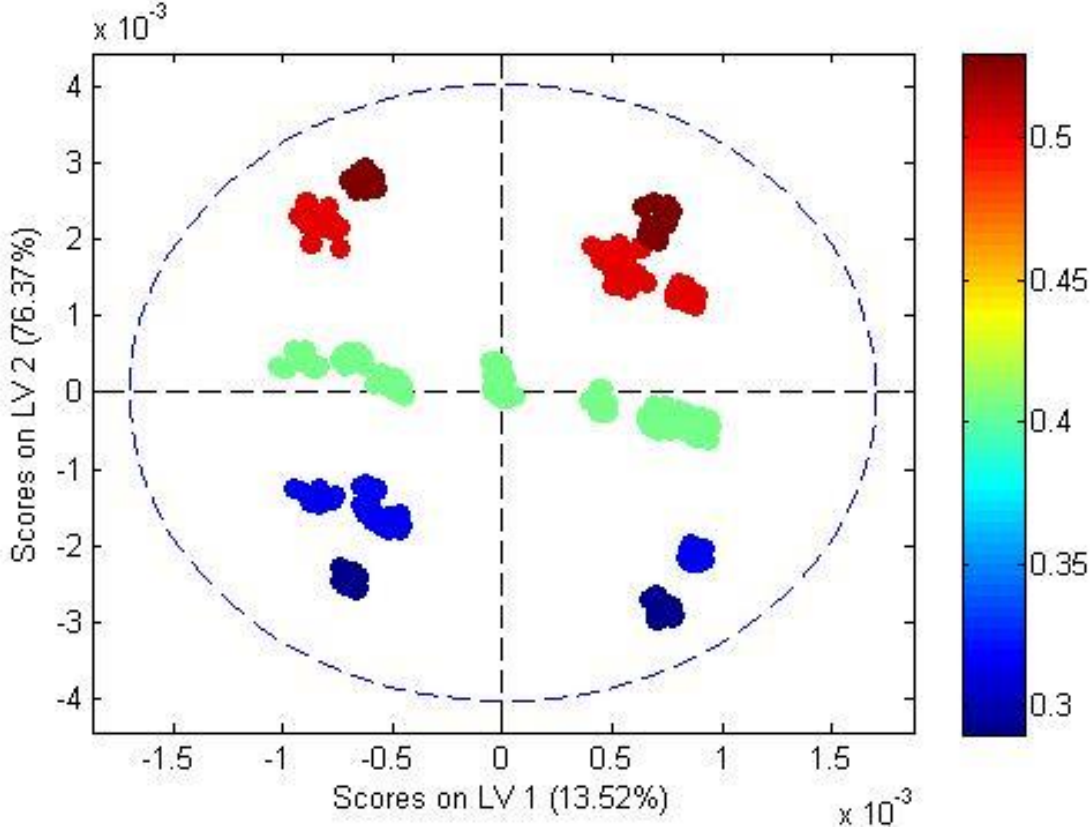
x 10^-3
Scores on LV 2 (76.37%)
Scores on LV 1 (13.52%)
x 10^-3
0.5
0.45
0.4
0.35
0.3

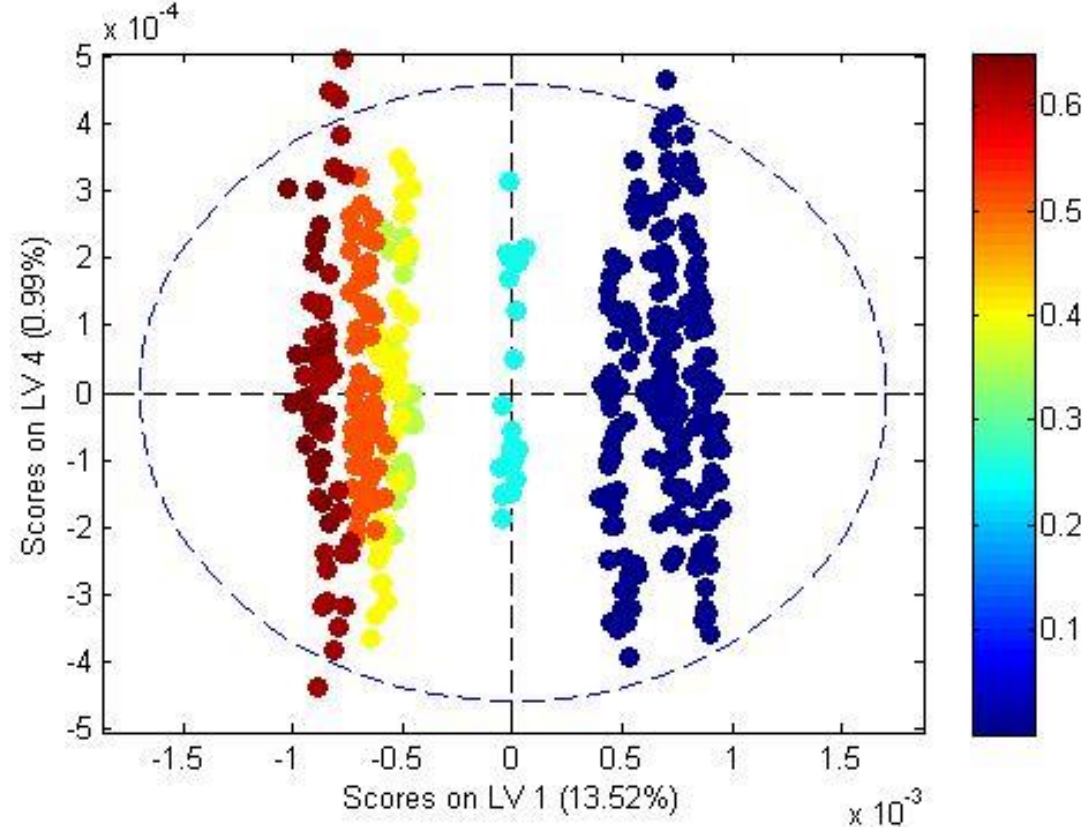
x 10^-4
Scores on LV 4 (0.99%)
Scores on LV 1 (13.52%)
x 10^-3
0.6
0.5
0.4
0.3
0.2
0.1

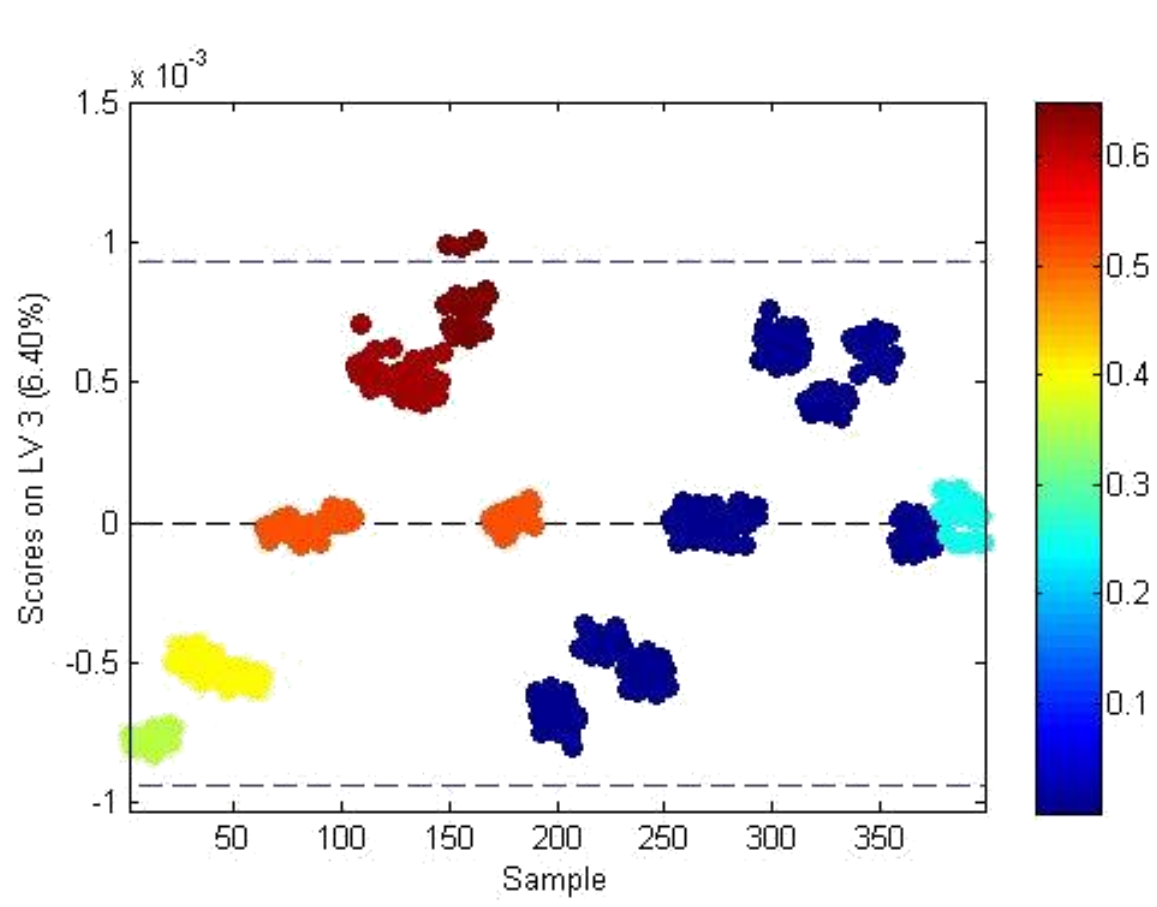
x 10^-3
1.5
1
0.5
0
-0.5
-1
Scores on LV 3 (6.40%)
50
100
150
200
250
300
350
Sample
0.6
0.5
0.4
0.3
0.2
0.1

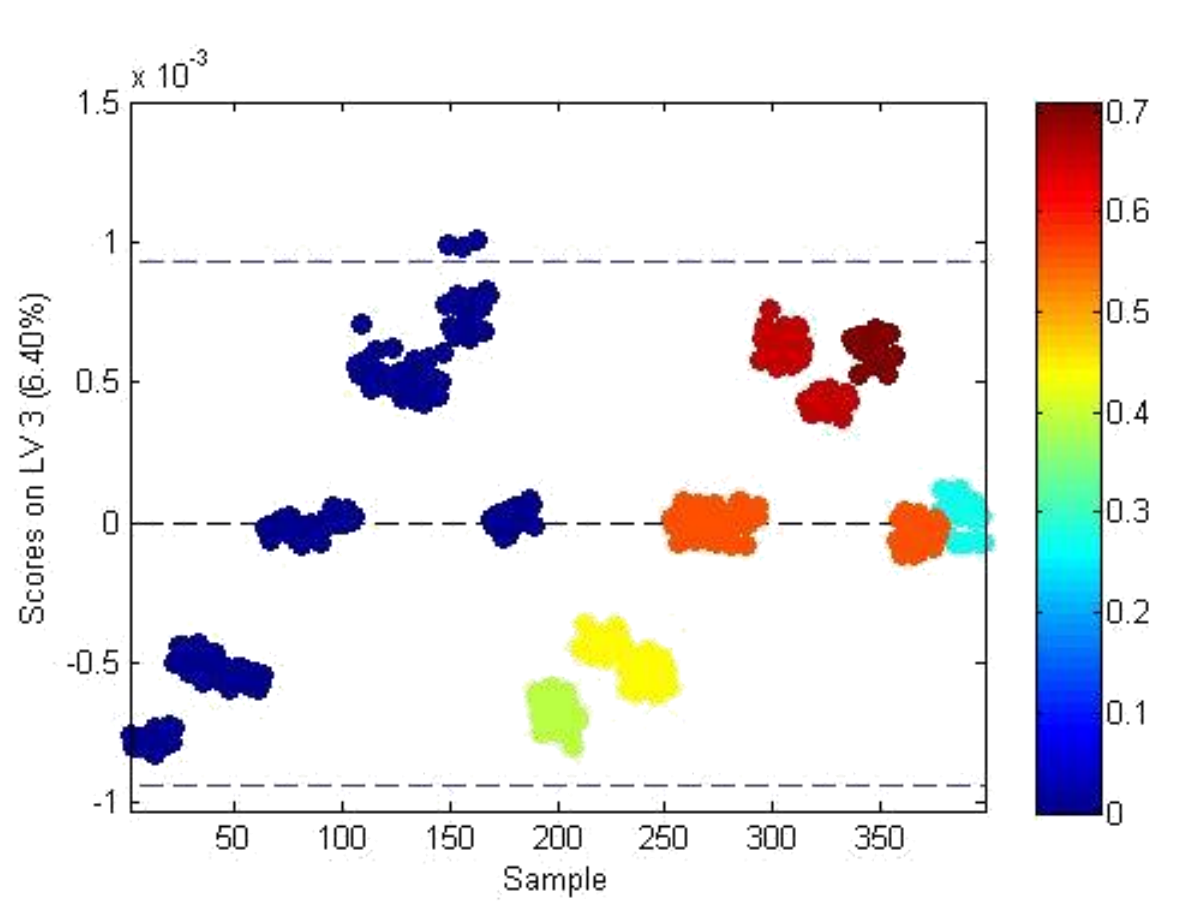
x 10^-3
1.5
1
0.5
0
-0.5
-1
Scores on LV 3 (6.40%)
50
100
150
200
250
300
350
Sample
0.7
0.6
0.5
0.4
0.3
0.2
0.1
0

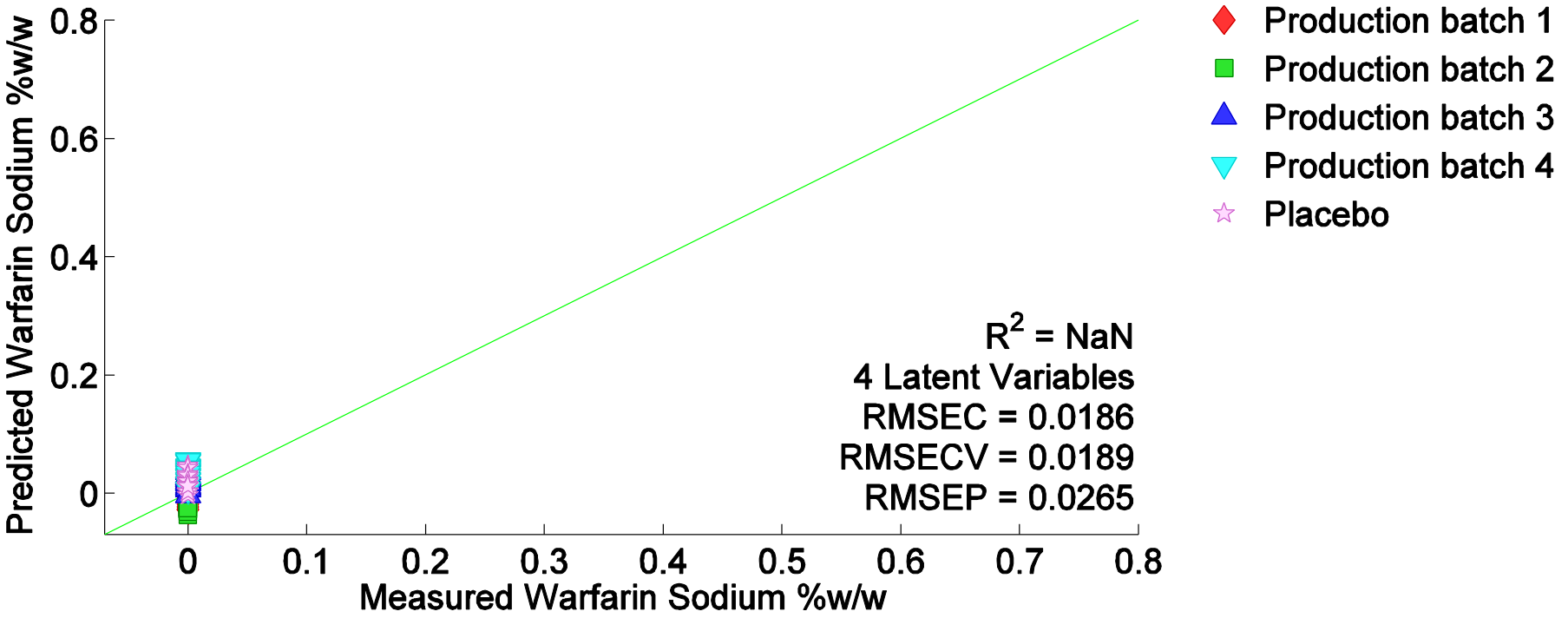
Production batch 1
Production batch 2
Production batch 3
Production batch 4
Placebo
Predicted Warfarin Sodium %w/w
Measured Warfarin Sodium %w/w
0
0.2
0.4
0.6
0.8
0.1
0.3
0.5
0.7
R2 = NaN
4 Latent Variables
RMSEC = 0.0186
RMSECV = 0.0189
RMSEP = 0.0265

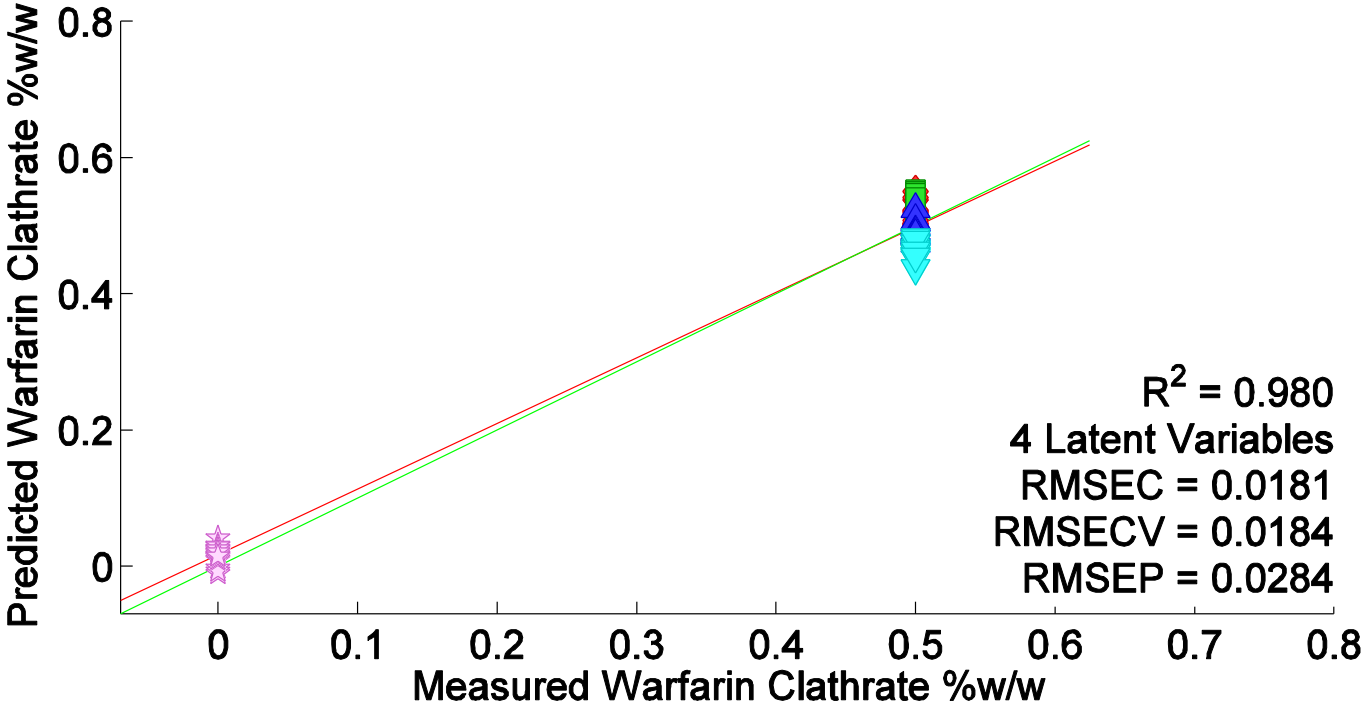
Predicted Warfarin Clathrate %w/w
Measured Warfarin Clathrate %w/w
0
0.2
0.4
0.6
0.8
0.1
0.3
0.5
0.7
R2 = 0.980
4 Latent Variables
RMSEC = 0.0181
RMSECV = 0.0184
RMSEP = 0.0284